



**HAL**  
open science

## Piezoresistive Effect in the $[\text{Fe}(\text{Htrz})_2(\text{trz})](\text{BF}_4)$ Spin Crossover Complex

Andrei Diaconu, Simona-Lacramioara Lupu, Ionela Rusu, Ioan-Marian Risca, Lionel Salmon, Gábor Molnár, Azzedine Bousseksou, Philippe Demont, Aurelian Rotaru

### ► To cite this version:

Andrei Diaconu, Simona-Lacramioara Lupu, Ionela Rusu, Ioan-Marian Risca, Lionel Salmon, et al.. Piezoresistive Effect in the  $[\text{Fe}(\text{Htrz})_2(\text{trz})](\text{BF}_4)$  Spin Crossover Complex. *Journal of Physical Chemistry Letters*, 2017, 8 (13), pp.3147-3151. <10.1021/acs.jpcclett.7b01111>. <hal-01556504>

**HAL Id: hal-01556504**

**<https://hal.science/hal-01556504v1>**

Submitted on 5 Jul 2017

HAL is a multi-disciplinary open access archive for the deposit and dissemination of scientific research documents, whether they are published or not. The documents may come from teaching and research institutions in France or abroad, or from public or private research centers.

L'archive ouverte pluridisciplinaire HAL, est destinée au dépôt et à la diffusion de documents scientifiques de niveau recherche, publiés ou non, émanant des établissements d'enseignement et de recherche français ou étrangers, des laboratoires publics ou privés.



HAL Authorization



## Open Archive TOULOUSE Archive Ouverte (OATAO)

OATAO is an open access repository that collects the work of Toulouse researchers and makes it freely available over the web where possible.

This is an author-deposited version published in : <http://oatao.univ-toulouse.fr/>  
Eprints ID : 18010

**To link to this article** : DOI: 10.1021/acs.jpcllett.7b01111  
URL : <http://dx.doi.org/10.1021/acs.jpcllett.7b01111>

**To cite this version** : Diaconu, Andrei and Lupu, Simona-Lacramioara and Rusu, Ionela and Risca, Ioan-Marian and Salmon, Lionel and Molnar, Gabor and Bousseksou, Azzedine and Demont, Philippe and Rotaru, Aurelian *Piezoresistive effect in the  $[Fe(Htrz)_2(trz)](BF_4)$  spin crossover complex*. (2017) The Journal of Physical Chemistry Letters, vol. 8. pp. 3147-3151. ISSN 1948-7185

Any correspondence concerning this service should be sent to the repository administrator: [staff-oatao@listes-diff.inp-toulouse.fr](mailto:staff-oatao@listes-diff.inp-toulouse.fr)

# Piezoresistive Effect in the $[\text{Fe}(\text{Htrz})_2(\text{trz})](\text{BF}_4)$ Spin Crossover Complex

Andrei Diaconu,<sup>†,‡</sup> Simona-Lacramioara Lupu,<sup>†,‡</sup> Ionela Rusu,<sup>†</sup> Ioan-Marian Risca,<sup>‡</sup> Lionel Salmon,<sup>§</sup> Gábor Molnár,<sup>§</sup> Azzedine Bousseksou,<sup>§</sup> Philippe Demont,<sup>||</sup> and Aurelian Rotaru<sup>\*,†</sup>

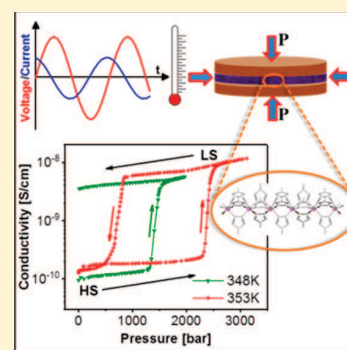
<sup>†</sup>Faculty of Electrical Engineering and Computer Science & Research Center MANSiD, Stefan cel Mare University, Suceava 720229, Romania

<sup>‡</sup>Faculty of Forestry & Research Center MANSiD, Stefan cel Mare University, Suceava 720229, Romania

<sup>§</sup>LCC, CNRS & Université de Toulouse (UPS, INP), Toulouse 31013, France

<sup>||</sup>Institute Carnot CIRIMAT, CNRS-INPT-UPS, Physique des Polymères, 118 route de Narbonne, Toulouse 31062, France

**ABSTRACT:** We report on the effect of hydrostatic pressure on the electrical conductivity and dielectric permittivity of the  $[\text{Fe}(\text{Htrz})_2(\text{trz})](\text{BF}_4)$  (Htrz = 1H-1,2,4-triazole) spin crossover complex. Variable-temperature and -pressure broad-band impedance spectrometry revealed a piezoresistive effect of more than 1 order of magnitude for pressures as low as 500 bar, associated with a large pressure-induced hysteresis of 1700 bar. The origin of the piezoresistive effect has been attributed to the pressure-induced spin state switching in the complex, and the associated  $P,T$  phase diagram was determined.



Bistable molecular complexes that can exist in two interchangeable states can act as switches under external stimuli. In this context, molecular spin crossover (SCO) compounds present a special interest due to their response to various external stimuli that might lead to a wide range of potential applications.<sup>1,2</sup> In these systems, the electronic configuration of the metal can be conveniently switched from the so-called low-spin (LS) to a high-spin (HS) electronic configuration in response to an external stimulus such as temperature, pressure, light irradiation, and so forth.<sup>3</sup> This spin state switching leads to a pronounced change of various material properties, including optical, magnetic, mechanical, and electrical characteristics. Because bulk SCO materials are in general highly insulating,<sup>4</sup> their electrical properties have been largely ignored and received growing interest only in the past few years, in parallel with the emergence of nanoscale SCO materials.<sup>5</sup> To date, most of the studies have been focused on the thermal bistability of the electrical properties.<sup>4–12</sup> A few studies have evidenced also remarkable switching of electrical transport properties under electrical stimuli<sup>12–15</sup> and light irradiation.<sup>16,17</sup>

Pressure is also a very useful parameter to control the spin state of these materials. Indeed, it is well-known that due to the substantial volume difference between the LS and HS states (typically between a 1 and 10% unit cell volume change), an applied pressure stabilizes the LS state.<sup>3</sup> In general, a  $\sim 10$ – $20$  K upshift of the spin transition is observed under an applied

hydrostatic pressure of 1 kbar.<sup>18–23</sup> This effect could be very useful in order to “push” the spin transition to higher temperatures where the thermal activation of charge carrier mobility should allow for higher conductivity. Besides the upshift of the spin transition temperature, pressure is also expected to increase the conductivity by itself due to the increasing density of the material, which is expected to enhance the charge carrier hopping rates.<sup>24</sup> In addition, at constant temperature, an applied pressure can also trigger the spin transition, leading, in some cases, to a pressure-induced bistability.<sup>25,26</sup>

To explore these potentially very useful phenomena, we carried out conductivity measurements as a function of temperature and pressure on the  $[\text{Fe}(\text{Htrz})_2(\text{trz})](\text{BF}_4)$  (1) spin crossover complex. At atmospheric pressure, this compound exhibits a pronounced conductivity switching when cycled around the spin transition temperature,<sup>6</sup> a phenomenon that was exploited in a series of micro- and nanoelectronic research devices.<sup>7–9,12</sup> This complex is somewhat unique among the spin crossover compounds, exhibiting a very large hysteresis loop above room temperature.<sup>27</sup> Nevertheless, the fact that this transition is very robust and

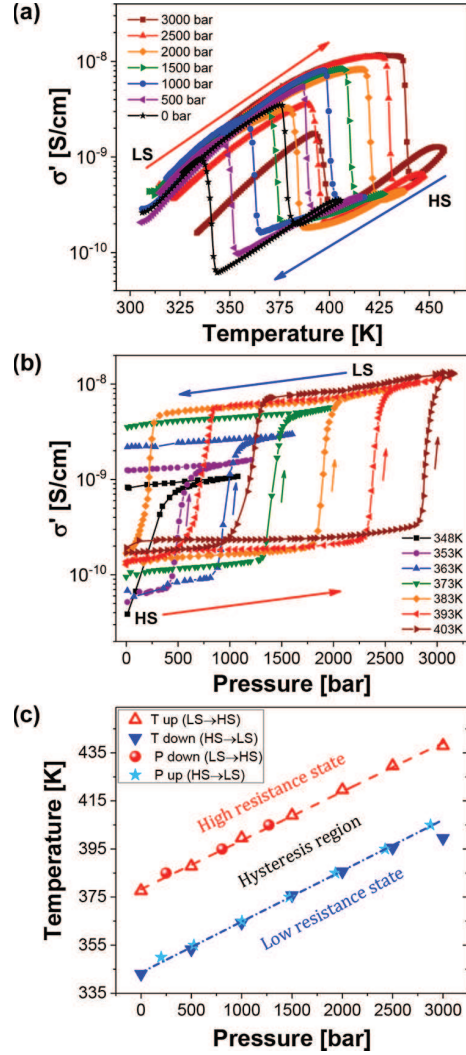
isostructural and that no lattice solvent is involved makes **1** a benchmark compound for different investigations.

Magnetic measurements were used to confirm the thermal SCO in a polycrystalline sample at around 365 K as well as the well-known thermal hysteresis of about 40 K width<sup>27</sup> (see Figures S2 and S3 in the Supporting Information (SI) for the magnetic data and other sample characterization details). The conductivity, the electric modulus, and the dielectric permittivity of the sample recorded at atmospheric pressure at different temperatures are also reported in the SI (Figures S4–S6) and are comparable to the data recorded on the same complex previously.<sup>28</sup> It should also be noted that, prior to the measurements under pressure, the good reproducibility of the spin transition was controlled over eight consecutive thermal cycles (Figure S7). For high-pressure measurements, the powder was slightly pressed to a thickness of 1.96 mm between two parallel electrodes of 15 mm diameter within a Teflon ring and sealed by epoxy glue so that no losses or changes in the thickness of the sample may occur. The electrodes were connected by flexible leads to high-pressure feedthrough connectors in a commercial high-pressure cell (Novocontrol Technologies). Silicone oil was used as a pressure-transmitting medium, and the electrode assembly, including the inner powder layer, was fully immersed in oil to provide hydrostatic conditions. It was confirmed that the silicone oil has negligible effect on the measured electrical signal. Pressure can be changed in small steps of  $\sim 10$  bar up to 3 kbar upon both compression and decompression. A schematic of the high-pressure setup is presented in the SI (Figure S1).

Of particular interest for the setup is the possibility to carry out pressure as well as temperature scans at fixed temperature and pressure values, respectively, providing a rather unique tool to explore the  $P,T$  phase diagram along different paths in a finely resolved manner. The complex impedance at fixed  $P,T$  values was measured using a Novocontrol BDS40 broad-band dielectric spectrometer by sweeping the frequency of the applied AC voltage ( $V_{\text{rms}} = 1$  V) between 0.1 Hz and 1 MHz.

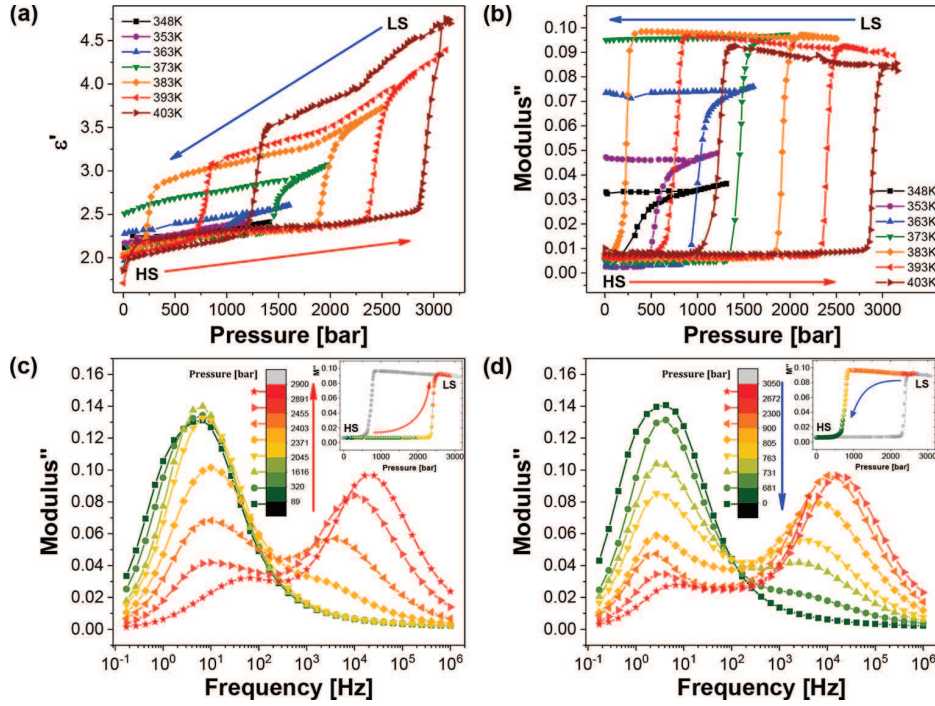
Figure 1a shows the temperature dependence of the real part of the AC conductivity (10 kHz) recorded between 300 and 450 K at fixed pressure values. The electrical conductivity displays a spin state dependence with a thermal hysteresis loop and a more conducting LS state. By applying an external pressure, a progressive shift of the thermal hysteresis loop toward higher temperatures is observed. When going from 1 atm to 3 kbar, the barycenter of the hysteresis is displaced from 355 to 415 K, while the hysteresis width ( $\sim 39$  K) remains nearly constant throughout the whole pressure range.

Figure 1b displays complementary experiments wherein the conductivity was measured at constant temperature values while sweeping the pressure between 1 atm and 3 kbar. For each curve, the temperature was first raised above 410 K, so that the sample switched to the HS state in order to make it possible to switch it back to the LS state by increasing the pressure. When the pressure was applied at a temperature above the LS  $\rightarrow$  HS transition temperature, it led to piezohysteresis loops, whose widths were virtually constant ( $\sim 1680$  bar). On the other hand, when the pressure was applied within the thermal hysteresis region, a piezoresistive switching effect was obtained, characterized by a sharp remnant drop of the resistance of more than 1 order of magnitude within a pressure range of  $\sim 500$  bar. Obviously, the origin of this remarkable piezoresistive effect is related to the pressure-induced spin state switching properties of the SCO complex **1**.



**Figure 1.** (a) Temperature dependence of the real part of the AC conductivity recorded at 10 kHz at various applied pressures, (b) pressure dependence of the electrical conductivity at 10 kHz recorded at various temperatures, and (c) the phase diagram in  $P,T$  coordinates. The dashed lines represent the linear fit of the data.

This can be better appreciated in the  $P-T$  phase diagram shown in Figure 1c, which was constructed using both temperature and pressure scan data. The perfect overlap between these data points highlights the outstanding stability of the spin transition during repeated cycling at high temperatures (up to 435 K) and high pressures (up to 3 kbar) simultaneously. Piezoresistive switching is possible within the hysteresis region, which is delimited by the coexistence lines. The slope of the cooling/compression coexistence line is  $\sim 21.2 \pm 0.5$  K/kbar, while that of the heating/decompression line is  $20.9 \pm 0.4$  K/kbar. The observed pressure-induced shift of the spin transition is somewhat lower than that reported previously for the same SCO complex studied by magnetic methods ( $29 \pm 7$  K/kbar)<sup>29</sup> but falls in the typical range expected for ferrous SCO complexes.<sup>19</sup> On the other hand, the virtually constant hysteresis width up to 3 kbar is a less common effect. In fact, mean-field theories predict a decrease of the hysteresis width with increasing pressure. This behavior has been observed in several SCO systems under hydrostatic pressure condi-



**Figure 2.** Pressure dependence of (a) the dielectric permittivity (real part) and (b) the electric modulus (imaginary part) recorded at 10 kHz for various temperatures. (c,d) Frequency dependence of the imaginary part of the electrical modulus recorded at 393 K for various pressure values in the loading and unloading modes. (Inset) Corresponding pressure hysteresis at 10 kHz.

tions.<sup>23,25,30</sup> However, the opposite behavior, that is, an increase of the hysteresis width with increasing pressure, has also been observed in various complexes and has been attributed either to the occurrence of a pressure-induced phase transition or to the anharmonicity of the lattice.<sup>20,31–33</sup> In the case of **1**, the Clapeyron slope can be estimated as  $dP/dT = \Delta S/\Delta V = 28 \pm 3$  K/kbar on the basis of reported entropy<sup>27</sup> and volume<sup>34</sup> changes associated with the SCO. The conventional mean-field Ising-like model of SCO<sup>35</sup> predicts also a linear increase of the transition temperature at a rate of 25 K/kbar, which is in reasonable agreement with the experiment. On the other hand, this theory predicts a monotonous decrease of the hysteresis width from 40 K at 1 atm to 20 K at 3 kbar (see the SI for more details on the model), which is not observed in our data. As discussed in ref 33, this discrepancy between experiment and theory is likely to occur due to the anharmonicity of the lattice and, in particular, the volume dependence of the bulk modulus.

Remarkably, the conductivity in the LS state exceeds with more than 1 order of magnitude that in the HS state throughout the whole range of applied pressures. The switching amplitude  $(\sigma'_{LS} - \sigma'_{HS})/\sigma'_{HS}$  slightly increases with pressure from  $\sim 15$  (1 atm) to  $\sim 30$  (3 kbar). This might be explained by an increase of the thermal activation energy of the conductivity in the HS state under pressure, while it remains nearly unchanged in the LS state (see Figures S8 and S9 in the SI). Another important finding is the significant increase of the conductivity of the sample near the spin transition for an applied external pressure of 3 kbar. As can be inferred from Figure 1a, the main contribution to this pressure-induced enhancement of the conductivity comes from the upshift of the spin transition temperature, which, in turn, leads to increased thermal activation of the charge transfer. Nevertheless, a clear intrinsic pressure effect on the conductivity can also be denoted

in the isothermal curves in Figure 1b. Similar to that observed in organic materials,<sup>24</sup> this latter effect most likely finds its origin in the enhanced overlap of the molecular orbitals under pressure, leading to higher charge carrier mobility (hopping rate).

The pressure effect on the dielectric properties has also been investigated. Figure 2a displays the pressure dependence of the real part of the dielectric permittivity recorded at selected temperatures (see also Figure S12 for the temperature scans at fixed pressures). Similar to the conductivity data,  $\epsilon'$  displays a pressure-induced hysteresis for temperatures above the hysteresis region, while a pressure-induced switching of  $\epsilon'$  can be obtained inside of the hysteresis. Contrary to the behavior of  $\sigma'$ , the switching amplitude of the dielectric constant  $(\epsilon'_{LS} - \epsilon'_{HS})/\epsilon'_{HS}$  increases considerably when increasing the pressure. To better understand the origin of this phenomenon, the data were also analyzed in the electric modulus formalism ( $M^* = 1/\epsilon^*$ ).<sup>28</sup> The data shown in Figures 2b and S12 suggest that the observed variation of  $\epsilon'$  is not entirely an intrinsic property of our sample but most likely altered by contributions from electrode and interface polarization effects. The modulus data also gives access to the characteristics of the charge carrier relaxation processes in the two spin states. Figure 2c,d shows the frequency dependence of the imaginary part of the electrical modulus  $M''$  during the compression and decompression processes, respectively. One can observe loss peaks at around 30 Hz and 30 kHz characteristic of the HS and LS states, respectively. As was discussed in ref 33, the higher relaxation (i.e., hopping) frequency in the LS state is perfectly in line with the higher conductivity of this phase. One can depict also a slight shift of the relaxation peaks (in a given spin state) toward higher frequencies, which can also be correlated with the pressure-

induced increase of the conductivity observed in Figure 1b. Hence, the pressure effect on the conductivity can be interpreted as an increase in charge carrier mobility.

In summary, we observed a significant pressure-induced increase of the conductivity in the spin crossover complex  $[\text{Fe}(\text{Htrz})_2(\text{trz})](\text{BF}_4)$  as well as a pronounced piezoresistive effect at the spin transition, accompanied by a large piezohysteresis loop. These results are likely generalizable to other SCO complexes and open up, therefore, new perspectives for technological applications such as pressure sensors and actuators with electrical output.

## ■ ASSOCIATED CONTENT

### 📄 Supporting Information

The Supporting Information is available free of charge on the ACS Publications website at DOI: 10.1021/acs.jpcllett.7b01111.

Details about the high-pressure experimental setup as well as details regarding synthesis and characterization, magnetic properties, and dielectric measurements under varying frequency, pressure, temperature, and time of the sample and a theoretical study based on the Ising-like model (PDF)

## ■ AUTHOR INFORMATION

### Corresponding Author

\*E-mail: aurelian.rotaru@usm.ro.

### ORCID

Gábor Molnár: 0000-0001-6032-6393

Aurelian Rotaru: 0000-0002-8782-7988

### Author Contributions

#A.D. and S.-L.L. contributed equally to this work.

### Notes

The authors declare no competing financial interest.

## ■ ACKNOWLEDGMENTS

This work was partially funded by the joint French–Romanian project ANR-UEFISCDI (Contracts 9ROFR/01.02.2013 and ANR-12-IS07-0003-01) and by the European Commission through the SPINSWITCH project (H2020-MSCA-RISE-2016, Grant Agreement No. 734322).

## ■ REFERENCES

- (1) Halcrow, M. A. *Spin-Crossover Materials. Properties and Applications*; John Wiley & Sons, Ltd., 2013.
- (2) Bousseksou, A.; Molnar, G.; Salmon, L.; Nicolazzi, W. Molecular Spin Crossover Phenomenon: Recent Achievements and Prospects. *Chem. Soc. Rev.* **2011**, *40*, 3313–3335.
- (3) Gütllich, P.; Hauser, A.; Spiering, H. Thermal and Optical Switching of Iron(II) Complexes. *Angew. Chem., Int. Ed. Engl.* **1994**, *33*, 2024–2054.
- (4) Bousseksou, A.; Molnar, G.; Demont, P.; Menegotto, J. Observation of a Thermal Hysteresis Loop in the Dielectric Constant of Spin Crossover Complexes: Towards Molecular Memory Devices. *J. Mater. Chem.* **2003**, *13*, 2069–2071.
- (5) Lefter, C.; Davesne, V.; Salmon, L.; Molnár, G.; Demont, P.; et al. Charge Transport and Electrical Properties of Spin Crossover Materials: Towards Nanoelectronic and Spintronic Devices. *Magnetochemistry* **2016**, *2*, 18.
- (6) Rotaru, A.; Gural'skiy, I. A.; Molnar, G.; Salmon, L.; Demont, P.; et al. Spin State Dependence of Electrical Conductivity of Spin Crossover Materials. *Chem. Commun.* **2012**, *48*, 4163–4165.
- (7) Rotaru, A.; Dugay, J.; Tan, R. P.; Gural'skiy, I. A.; Salmon, L.; et al. Nano-Electromanipulation of Spin Crossover Nanorods: Towards Switchable Nanoelectronic Devices. *Adv. Mater.* **2013**, *25*, 1745–1749.
- (8) Dugay, J.; Gimenez-Marques, M.; Kozlova, T.; Zandbergen, H. W.; Coronado, E.; et al. Spin Switching in Electronic Devices Based on 2D Assemblies of Spin-Crossover Nanoparticles. *Adv. Mater.* **2015**, *27*, 1288–1293.
- (9) Dugay, J.; Aarts, M.; Giménez-Marqués, M.; Kozlova, T.; Zandbergen, H. W.; et al. Phase Transitions in Spin-Crossover Thin Films Probed by Graphene Transport Measurements. *Nano Lett.* **2017**, *17*, 186–193.
- (10) Bovo, G.; Braunlich, I.; Caseri, W. R.; Stingelin, N.; Anthopoulos, T. D.; et al. Room Temperature Dielectric Bistability in Solution-Processed Spin Crossover Polymer Thin Films. *J. Mater. Chem. C* **2016**, *4*, 6240–6248.
- (11) Zhang, X.; Palamarciuc, T.; Letard, J.-F.; Rosa, P.; Lozada, E. V.; et al. The Spin State of a Molecular Adsorbate Driven by the Ferroelectric Substrate Polarization. *Chem. Commun.* **2014**, *50*, 2255–2257.
- (12) Prins, F.; Monrabal-Capilla, M.; Osorio, E. A.; Coronado, E.; Van der Zant, H. S. J. Room-Temperature Electrical Addressing of a Bistable Spin-Crossover Molecular System. *Adv. Mater.* **2011**, *23*, 1545–1549.
- (13) Gopakumar, T. G.; Matino, F.; Naggert, H.; Bannwarth, A.; Tuzek, F.; et al. Electron-Induced Spin Crossover of Single Molecules in a Bilayer on Gold. *Angew. Chem., Int. Ed.* **2012**, *51*, 6262–6266.
- (14) Miyamachi, T.; Gruber, M.; Davesne, V.; Bowen, M.; Boukari, S.; et al. Robust Spin Crossover and Memristance Across a Single Molecule. *Nat. Commun.* **2012**, *3*, 938.
- (15) Gueddida, S.; Gruber, M.; Miyamachi, T.; Beaurepaire, E.; Wulfhekel, W.; et al. Exchange Coupling of Spin-Crossover Molecules to Ferromagnetic Co Islands. *J. Phys. Chem. Lett.* **2016**, *7*, 900–904.
- (16) Lefter, C.; Rat, S.; Costa, J. S.; Manrique-Juárez, M. D.; Quintero, C. M.; et al. Current Switching Coupled to Molecular Spin-States in Large-Area Junctions. *Adv. Mater.* **2016**, *28*, 7508–7514.
- (17) Bairagi, K.; Iasco, O.; Bellec, A.; Kartsev, A.; Li, D.; et al. Molecular-Scale Dynamics of Light-Induced Spin Crossover in a Two-Dimensional Layer. *Nat. Commun.* **2016**, *7*, 12212.
- (18) Slichter, C. P.; Drickamer, H. G. Pressure-Induced Electronic Changes in Compounds of Iron. *J. Chem. Phys.* **1972**, *56*, 2142–2160.
- (19) Boillot, M. L.; Zarembowitch, J.; Itié, J. P.; Polian, A.; Bourdet, E.; et al. Pressure-Induced Spin-State Crossovers at Room Temperature in Iron(II) Complexes: Comparative Analysis; a XANES Investigation of Some New Transitions. *New J. Chem.* **2002**, *26*, 313–322.
- (20) Ksenofontov, V.; Spiering, H.; Schreiner, A.; Levchenko, G.; Goodwin, H. A.; et al. The Influence of Hydrostatic Pressure on Hysteresis Phase Transition in Spin Crossover Compounds. *J. Phys. Chem. Solids* **1999**, *60*, 393–399.
- (21) Jęftić, J.; Hauser, A. The HS→LS Relaxation Under External Pressure in the Fe(II) Spin-Crossover System  $[\text{Zn}_{1-x}\text{Fe}_x(\text{ptz})_6](\text{BF}_4)_2$  (ptz = 1-propyltetrazole; x = 0.1). *Chem. Phys. Lett.* **1996**, *248*, 458–463.
- (22) Gütllich, P.; Gaspar, A. B.; Garcia, Y.; Ksenofontov, V. Pressure Effect studies in molecular magnetism. *C. R. Chim.* **2007**, *10*, 21–36.
- (23) Rotaru, A.; Linares, J.; Varret, F.; Codjovi, E.; Slimani, A.; et al. Pressure effect investigated with first-order reversal-curve method on the spin-transition compounds  $\text{Fe}_x\text{Zn}_{1-x}(\text{btr})_2(\text{NCS})_2\cdot\text{H}_2\text{O}$  (x = 0.6; 1). *Phys. Rev. B: Condens. Matter Mater. Phys.* **2011**, *83*, 224107.
- (24) Okada, Y.; Sakai, K.; Uemura, T.; Nakazawa, Y.; Takeya, J. Charge transport and Hall effect in rubrene single-crystal transistors under high pressure. *Phys. Rev. B: Condens. Matter Mater. Phys.* **2011**, *84*, 245308.
- (25) Codjovi, E.; Menendez, N.; Jęftić, J.; Varret, F. Pressure and temperature hysteresis in the spin-transition solid  $\text{Fe}(\text{btr})_2(\text{NCS})_2\cdot\text{H}_2\text{O}$ ; pure and diluted in Ni matrix. *C. R. Acad. Sci., Ser. IIC: Chim.* **2001**, *4*, 181–188.
- (26) Molnar, G.; Niel, V.; Real, J. A.; Dubrovinsky, L.; Bousseksou, A.; et al. Raman spectroscopic study of pressure effects on the spin-crossover coordination polymers  $\text{Fe}(\text{pyrazine})[\text{M}(\text{CN})_4]\cdot 2\text{H}_2\text{O}$  (M =

Ni; Pd; Pt). First observation of a piezo-hysteresis loop at room temperature. *J. Phys. Chem. B* **2003**, *107*, 3149–3155.

(27) Kröber, J.; Audiere, J. P.; Claude, R.; Codjovi, E.; Kahn, O.; et al. Spin Transition and Thermal Hysteresis in the Molecular-Based Materials  $[\text{Fe}(\text{Htrz})_2(\text{trz})](\text{BF}_4)$  and  $[\text{Fe}(\text{Htrz})_3](\text{BF}_4)_2 \cdot \text{H}_2\text{O}$  (Htrz = 1,2,4-4H-triazole, trz = 1,2,4-triazolato). *Chem. Mater.* **1994**, *6*, 1404–1412.

(28) Lefter, C.; Gural'skiy, I. A.; Peng, H.; Molnár, G.; Salmon, L.; et al. Dielectric and Charge Transport Properties of the Spin Crossover Complex  $[\text{Fe}(\text{Htrz})_2(\text{trz})](\text{BF}_4)$ . *Phys. Status Solidi RRL* **2014**, *8*, 191–193.

(29) Herrera, M. J.; Titos-Padilla, S.; Pope, S. J. A.; Berlanga, I.; Zamora, F.; et al. Studies on Bifunctional Fe(II)-triazole Spin Crossover Nanoparticles: Time-Dependent Luminescence; Surface Grafting and the Effect of a Silica Shell and Hydrostatic Pressure on the Magnetic Properties. *J. Mater. Chem. C* **2015**, *3*, 7819–7829.

(30) Jefic, J.; Menendez, N.; Wack, A.; Codjovi, E.; Linares, J.; et al. A Helium-Gas-Pressure Apparatus with Optical-Reflectivity Detection Tested with a Spin-Transition Solid. *Meas. Sci. Technol.* **1999**, *10*, 1059–1064.

(31) Gütlich, P.; Ksenofontov, V.; Gaspar, A. B. Pressure Effect Studies on Spin Crossover Systems. *Coord. Chem. Rev.* **2005**, *249*, 1811–1829.

(32) Ksenofontov, V.; Levchenko, G.; Spiering, H.; Gütlich, P.; Létard, J. F.; et al. Spin Crossover Behavior Under Pressure of  $\text{Fe}(\text{PM-L})_2(\text{NCS})_2$  Compounds with Substituted 2'-pyridylmethylene 4-anilino Ligands. *Chem. Phys. Lett.* **1998**, *294*, 545–553.

(33) Spiering, H.; Boukheddaden, K.; Linares, J.; Varret, F. Total free energy of a spin-crossover molecular system. *Phys. Rev. B: Condens. Matter Mater. Phys.* **2004**, *70*, 184106.

(34) Grosjean, A.; Negrier, P.; Bordet, P.; Etrillard, C.; Mondieig, D.; et al. Crystal Structures and Spin Crossover in the Polymeric Material  $\text{Fe}(\text{Htrz})_2(\text{trz})(\text{BF}_4)$  Including Coherent-Domain Size Reduction Effects. *Eur. J. Inorg. Chem.* **2013**, *2013*, 796–802.

(35) Bousseksou, A.; Nasser, J.; Linares, J.; Boukheddaden, K.; Varret, F. Ising-like Model for the 2-Step Spin Crossover. *J. Phys. I* **1992**, *2*, 1381–1403.